IEEE Access
Multidisciplinary | Rapid Review | Open Access Journal

Date of publication xxxx 00, 0000, date of current version xxxx 00, 0000.

Digital Object Identifier 10.1109/ACCESS.2018.DOI

Radio Source Localization in Multipath Channels Using EM Lens Assisted Massive Antennas Arrays

SARMAD A. SHAIKH[1] AND ANDREA M. TONELLO[1] (Senior Member, IEEE)
[1]Institute of Networked and Embedded Systems, University of Klagenfurt, Klagenfurt 9020, Austria

Corresponding author: A. M. Tonello (e-mail: andrea.tonello@aau.at).

This work was carried out at the University of Klagenfurt, Klagenfurt, Austria. S.A. Shaikh was supported by the Higher Education Commission (HEC) Pakistan and OeAD Austria under the scholarship program HRDI-UESTP-Austria (Code 050). S.A. Shaikh is now with the Department of Avionics Engineering, PAF-Karachi Institute of Economics and Technology (KIET), Karachi, Pakistan (e-mail: sarmad@pafkiet.edu.pk).

ABSTRACT The focusing ability of the lens antennas can significantly contribute to perform precise radio localization with low complexity in a massive antennas array (MAA) system. Thus, by combining lens antennas with a MAA, we propose an approach for radio source localization through angle of arrival (AoA) estimation in a multipath propagation scenario. We discuss two simplified antenna selection techniques to select and process the focused subsets of antennas. Then, we implement a low complexity time of arrival estimation scheme to detect the first arrival path (FAP) that contains the actual AoA information. Finally, the FAP signal is processed to estimate the AoA very efficiently, by applying one of the traditional subspace based methods. To simplify further the system architecture with only slight degradation in performance, we also propose a mixed analog-digital AoA estimation structure based on the application of the sum-difference signal patterns technique. The simulated root mean squared error performance curves as a function of the signal-to-noise-ratio demonstrate that the proposed approach is capable of providing good AoA estimation results while considerably reducing the overall system complexity as compared to the MAA system without the lens.

INDEX TERMS Angle of arrival estimation, electromagnetic lens antennas, localization, massive antennas array, massive MIMO, mixed analog-digital structure, sum-difference localization technique.

I. INTRODUCTION

The development of electromagnetic (EM) lens antennas has been driven from the extensive work on optics. The EM lenses have recently attracted a renewed interest by the wireless communications community due to the growing interest in developing high-frequency systems (i.e., millimeter wave), where the lens physical dimensions have acceptable size [1]–[3]. Because of their focusing property, the lens antennas are a good option for those wireless systems which utilize MAA technology, for instance, massive multiple-input-multiple-output (MIMO) systems for 5G networks. MAA systems offer advantages in spectral efficiency [4]–[6]. However, they have brought some challenging issues to be tackled. They include the need of a large amount of hardware RF chains, and processing of a big amount of data, which consequently increases the complexity and the power consumption of the system [4], [7]–[10].

Many solutions have been proposed in the relevant literature to tackle these challenges such as traditional antenna selection and combining schemes, mentioned in [7], [8] and the references therein, where one has to compromise between performance and complexity. Additionally, authors in [9], [11], [12] propose the EM lens-focusing antennas concept, where the signal energy is focused in a certain small subset of antenna elements as a function of the incidence angle. The focusing property of the EM lens can reduce the number of antenna element signals to be processed in baseband (BB), and therefore the overall hardware and computational complexity. Furthermore, it can provide advantages in reducing multipath propagation effects and thus supporting high data rate transmission in MAA systems. However, most of the literature studies data transmission aspects and not the application to radio localization as we do in this paper.

The radio localization can be performed using three well-

This article has been accepted for publication in a future issue of this journal, but has not been fully edited. Content may change prior to final publication. Citation information: DOI 10.1109/ACCESS.2019.2891110, IEEE Access

known techniques: 1) time of arrival (ToA) or time-difference-of-arrival (TDoA) which computes the wave propagation delay and consequently computes the distance between the transmitter and receiver [13]; 2) AoA or direction-of-arrival (DoA) estimation, which estimates the angle of the received signal that impinges on an antenna array [14], [15]; and 3) received signal strength indicator (RSSI), where estimation is carried out using the received signal strength by exploiting a propagation-loss model [16].

Extending our previous contribution in [17], in this work, we consider the localization in multipath channels based on AoA estimation with the exploitation of a MAA system. To perform the localization using the MAA system, few techniques have been reported in the existing relevant literature. For example, the authors in [18] and [19] estimate the DoA using the traditional method named estimation of signal parameter via rotational invariance (ESPRIT), where all the antenna elements of the system are considered. However, reduction in the complexity of the hardware implementation has not been explored in this work. Hybrid analog-digital and digital-analog techniques for DoA estimation in large antennas array system have been proposed in [20] with reduced computational complexity. Whereas authors consider the single user and line-of-sight (LoS) scenario only. A method for direct localization for massive MIMO in a multipath propagation environment has been proposed in [21]. It is based on the compressed sensing framework. Although this method performs well in performing the AoA and ToA estimation, it requires the same number of RF chains as the total number of antennas in the array. Moreover, tensor and deep learning based DoA estimation techniques with massive MIMO, proposed in [22] and [23], respectively, are not free from hardware and computational complexity. Additionally, the Gaussian process regression method in [24] has been proposed to find the position through fingerprints which require the prior knowledge of the area of operation and sophisticated comparison matching algorithms. Furthermore, citations [14] and [24], and the references therein indicate other localization methods such as proximity-based localization which is not free from complexities as it requires many base stations (BS's).

Herein, we present an approach to perform precise localization in a single source multipath propagation scenario using an EM lens assisted MAA system. We demonstrate that by exploiting the property of the EM lens to focus the received signal energy in a small subsets of antennas of a large uniform linear array (ULA), the source localization can be performed efficiently with reduced hardware and signal processing complexity. The main contributions of this paper are highlighted below.

- First, we introduce the system model for localization in a multipath environment using the EM lens assisted MAA structure, which is not available in the related literature work, according to the authors' knowledge. For this, a detailed system model using a fully digital/mixed analog-digital structure is presented to express the focusing ability of the EM lens in performing the radio source localization.
- Second, the EM lens antenna is discussed and characterized by EM field simulation using two materials, namely, silicon and quartz, aiming to relate the focusing area to the lens geometric parameters. Moreover, we present a lens based signal model for performing the localization using a very small subset of antennas, i.e., two-three antenna elements. More specifically, we describe the signal model in terms of the lens geometric parameters and angle of incidence, which contributes to separating the multipath components of a signal arriving from distinct directions.
- By using this distinctive focusing property, we introduce two antenna selection algorithms for processing the signals in the fully digital BB domain and in the mixed analog-digital RF domain, respectively. Furthermore, to implement the AoA estimation, initially we detect the subset of antennas that contains the first arrival path (FAP) and isolate the FAP itself via ToA estimation. This is followed by the AoA estimation technique, i.e., fully digital subspace based algorithm.
- Finally, in order to simplify further the computational complexity, we also implement a simple AoA finding technique that exploits sum $\left(\sum\right)$-difference $\left(\Delta\right)$ signal patterns of two antenna elements in the mixed analog-digital structure. It fits well in the proposed methodology and can be implemented with simple RF couplers.

The rest of the paper is organized in the following manner. Section II presents the proposed system model of the EM lens assisted MAA system. By briefly discussing the focusing ability of the lens antennas as a function of lens geometric parameters and angle of incidence, we provide the signal model for the proposed system in Section III. The lens based antenna selection and localization processes are explained in Section IV using the subspace and $\sum -\Delta$ patterns methods. The simulation results observed and parameters assumed, are provided in Section V with complexity and hardware reduction analysis. Finally, we conclude the paper in Section VI.

Notations: Boldface upper and lower case letters represent the matrices and vectors, respectively. Italic letters denote the scalars. Transpose of the matrix is given by $[.]^T$. The expectation operator is expressed as $\mathbb{E}[.]$.

II. SYSTEM MODEL

The proposed method for localization is based on the estimation of the AoA of the received signal. We consider a single-input multiple-output (SIMO) and single cell uplink transmission system where the BS consists of a large ULA. The antenna array is assumed to be placed in the vertical y-axis and centered at zero, and the field of view is -π/3 to +π/3 for practical reasons. Furthermore, we propose to combine the EM lens with the ULA consisting of M antenna elements, as shown in Fig. 1. The reason for integrating the EM lens

This article has been accepted for publication in a future issue of this journal, but has not been fully edited. Content may change prior to final publication. Citation information: DOI 10.1109/ACCESS.2019.2891110, IEEE Access

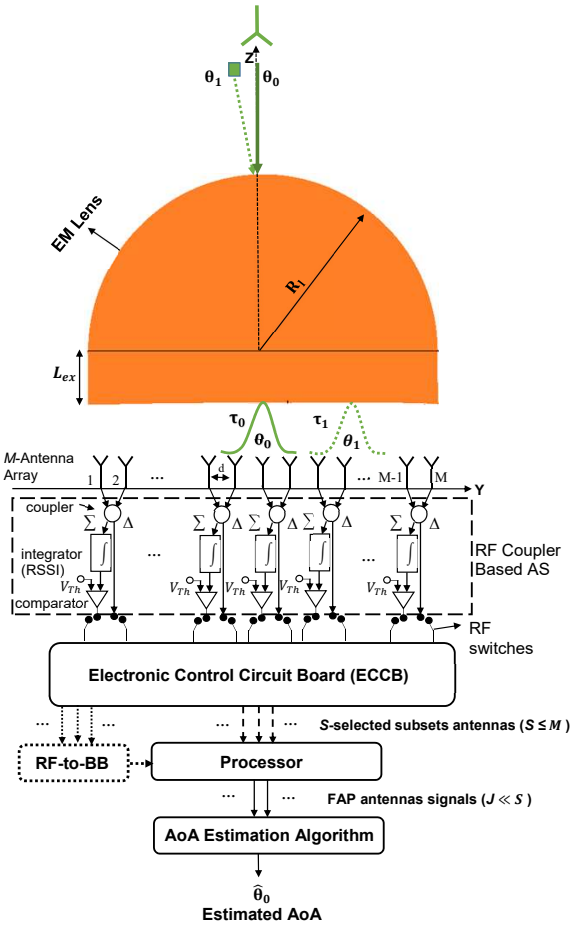

FIGURE 1: Design overview of the proposed system model. Dotted (. . .) line represents the digital structure. Dashed (− −) line denotes the mixed analog-digital structure.

with the ULA is that the EM lens has the ability to focus the received signal energy on a certain small area of the ULA and therefore to excite a subset of antenna elements as a function of the incidence angle (θ). As a result, it provides the advantage of reducing the number of RF chains to be used and signals to be processed. It also enables to separate the multipath components arriving from different directions [11]. Moreover, a fully digital BB or a mixed analog-digital structure can be realized aiming at increasing precision and simplifying the system further.

The proposed system model in Fig. 1 shows that as the incidence angle θ of the incoming multipath signal changes, the focused EM energy distribution on the subset (peak power location) sweeps accordingly on the ULA. Additionally, the average total obtained signal energy on the subset remains the same as w/o EM lens which is advantageous. This is because the EM lens only changes the received signal's energy distribution on the ULA. Moreover, the number of J excited antennas in a subset depends on the geometric design of the EM lens and consequently to the 3-dB beamwidth, as it is discussed in the next section.

To proceed, an appropriate antenna selection strategy is implemented followed by the application of an AoA estimation algorithm, namely, a fully digital subspace based strategy or a mixed analog-digital $\sum -\Delta$ processing strategy, on the excited subset's signal. These techniques will be discussed in detail in Section IV. In the following section, we will briefly describe the lens antenna design fundamentals followed by the resultant signal model for the proposed system design.

III. EM LENS ANTENNA AND SIGNAL MODEL

A. EM LENS ANTENNA

In this section, we describe how geometry and materials affect the EM lens. To design an efficient EM lens antenna, it is necessary to select a proper lens geometry (spherical/Luneburg, extended hemispherical, elliptic, and so on) and the lens material (teflon, rexolite, polyethylene, silicon, quartz, etc) [1], [25]. As shown in Fig. 1, the design geometric parameters of an extended hemispherical (EHS) lens mainly include the radius (R_l), extension length (L_{ex}) and the dielectric material's relative permittivity constant (ϵ_r), which actually controls the antenna parameters and focusing area, i.e., directivity and 3dB-beamwidth. Whereas, the directivity of an antenna is defined as the ratio of the radiation intensity in a certain direction to the average radiation intensity in unwanted directions (side lobes), and the 3dB-beamwidth (χ) is the angular separation between two points on the main beam lobe where the beam of the power pattern equals one half of the maximum value [26]. Typically, the values of R_l and ϵ_r for an EHS lens can be chosen in the range of R_l = $5\lambda_0$ to $25\lambda_0$, and ϵ_r =1.2 to 13, respectively, where λ_0 is the signal wavelength at central frequency f_0. While L_{ex} depends on the material chosen and the desired degree of focusing ability. Furthermore, the lenses made of dielectric materials, such as silicon (Si) and quartz (Qu), can improve the antenna performance significantly, and possess strong mechanical rigidity that enables the integration with microwave circuits using micro-electro-mechanical systems technology [1].

As an example, we can consider an EHS lens by using the Si and Qu materials and integrate it with the quarter wave transformer (QWT) fed patch antenna. Considered design parameters are $f_0 = 10$ GHz, R_l = $(11.4\lambda_0)/2$, L_{ex}=$0.22R_l$ for Si material ($\epsilon_r = 11.9$), and L_{ex}=$0.7R_l$ for Qu material ($\epsilon_r = 3.75$). Finally, 3D EM field simulations provide the values of directivity, side lobe levels, and χ as 25 (28.8) dBi, -17.1 (-16) dB, and $8.7^{\circ}(5.6^{\circ})$ for Si (Qu), respectively. Due to low ϵ_r and high L_{ex}, the Qu lens offers better results as compared to the Si lens. However, in practice, it requires manual adjustments in the geometry to achieve the desired performance level.

Additionally, Fig. 2 shows the obtained 2D directivity radiation patterns as a function of angle θ, for the designed Si and Qu lenses. Clearly, all these obtained results show an improvement w.r.t. a typical patch antenna without lens which on average can provide the directivity and χ as 6 dBi and 80^0,

This article has been accepted for publication in a future issue of this journal, but has not been fully edited. Content may change prior to final publication. Citation information: DOI 10.1109/ACCESS.2019.2891110, IEEE Access

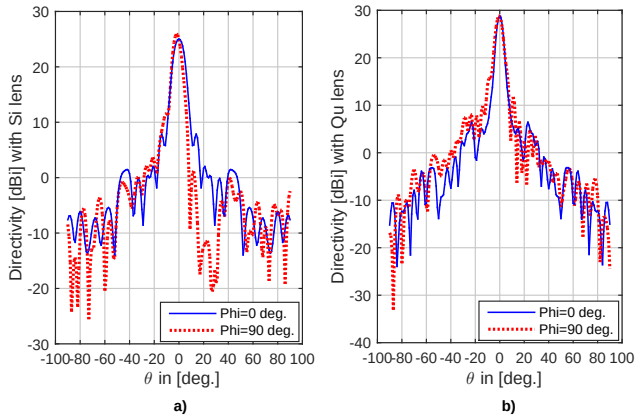

FIGURE 2: 2D far field directivity radiation patterns of the a) Si and b) Qu lens, at incidence signal angle $\theta_0 = 0^0$ and 90^0.

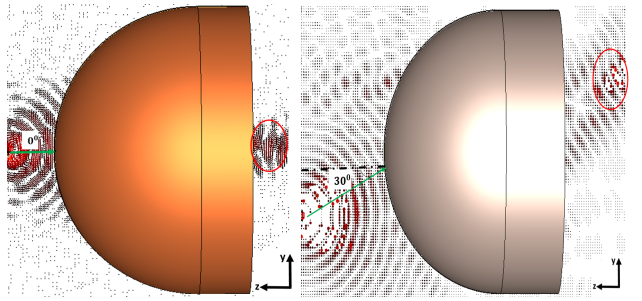

(a) (b)

FIGURE 3: E-field distribution with incidence angles of a) 0°(Si lens); and b) 30°(Qu lens).

respectively (design parameters of the assumed patch antenna are given in Appendix A). Moreover, the E-field distribution is also provided in Fig. 3 which shows that as the incidence angle θ_0 of the focused signal varies, the location distribution of the strongest E-field sweeps accordingly.

By extrapolating data from the EM simulations, we have been able to define the following relation for χ as a function of EHS lens geometric parameters:

$$\chi(R_l, L_{ex}, \epsilon_r) = \chi_0 + \omega\frac{R_l}{L_{ex}} - \varpi\sqrt{\epsilon_r}, \qquad (1)$$

where $\chi_0 = 70\lambda_0/D$ is the typical aperture antenna's 3dB-beamwidth, D represents the lens diameter ($D = 2R_l$), ω and ϖ are the constants that are equal to 1 in our setup. For simplicity, in the remainder of the paper, we refer to χ as the lens focusing design constant which provides the excited subset's size. Hence, by adjusting the lens's geometric parameters, the desired value of χ can be obtained which is an important parameter in the signal model as discussed in the rest of the paper.

B. SIGNAL MODEL

Let us consider a user terminal with one omnidirectional antenna that transmits a narrowband signal towards a BS consisting of an EM lens large ULA with M antenna elements, where $M \approx D/d$ is an even number and d is the spacing between two antennas in the ULA. The transmitted signal undergoes multipath propagation, so that the received signal after passing through the EM lens (i.e., EHS), impinges as a plane wave on small subsets of the ULA. Assuming multipath propagation with N_P paths, in some cases, distinct antenna subsets are excited by distinct multipath components, each with an AoA θ_p. Thus, the received signal on the m^{th} antenna of the ULA can be expressed as

$$z_m(t) = \sum_{p=1}^{N_P} P_m(R_l, L_{ex}, \epsilon_r, \theta_p) h_{mp} s(t - \tau_p) + n(t), \quad (2)$$

where s(t), $0<t<T_0$, is the transmitted signal with the bandwidth B and duration T_0 (assumed to be known at the BS). τ_p represents the time delay of the p^{th} multipath component, where τ_0 denotes the delay of the FAP/LoS component that is assumed to be always present. n(t) shows the additive white Gaussian noise with mean and variance of μ and σ, respectively. Furthermore, h_{mp} is the channel gain of the m^{th} antenna and p^{th} multipath component, which is defined as

$$h_{mp} = \alpha_p \exp\left(j\psi_p + j\frac{2\pi d}{\lambda_0}(m-1)\sin\theta_p\right), \qquad (3)$$

where α_p represents the channel attenuation of the p^{th} component. j and ψ_p, respectively, denote the imaginary term and the arrival signal phase of the p^{th} component which can be modeled as a random variable with a uniform distribution over [0, 2π]. Furthermore, the AoA θ_p of path p can be expressed as $\theta_p = \theta_0 \pm \eta_p$, where $\theta_0 \in [-\phi, \phi]$ is the actual AoA of the user terminal's location, and $\phi = \pi/3$ represents the maximum field of view of the array. While η_p denotes the offset with respect to the LoS component with angle θ_0.

Moreover, the parameter $P_m(R_l, L_{ex}, \epsilon_r, \theta_p)$ in (2) is the lens factor. It provides the power distribution of the received p^{th} path signal on a certain antennas subset of the ULA focused by the EM lens as a function of the lens design parameters $(R_l, L_{ex}, \epsilon_r)$ and incidence angle θ_p. Whereas, $P_m(R_l, L_{ex}, \epsilon_r, \theta_p)/M$ reflects the power fraction obtained by m^{th} antenna element. The lens factor can be obtained by integrating a power density function $f(a;\theta)$, as

$$P_m(R_l, L_{ex}, \epsilon_r, \theta) = c_0 \int_{a_m - d/2}^{a_m + d/2} f(a;\theta)da, \mid m - m^*(\theta) \mid \leq \chi, \qquad (4)$$

where $m^*(\theta)$ denotes the AoA-based peak power location index of an excited subset whose size is determined by χ in (1) as a function of the lens design parameters. Furthermore, c_0 is a constant such that $\sum_{m=1}^{M} P_m(R_l, L_{ex}, \epsilon_r, \theta) = M$, and a_m represents the m^{th} antenna index of the ULA at the BS, which can be defined as

$$a_m = (m-1)d - \left(\frac{(M-1)d}{2}\right). \qquad (5)$$

This article has been accepted for publication in a future issue of this journal, but has not been fully edited. Content may change prior to final publication. Citation information: DOI 10.1109/ACCESS.2019.2891110, IEEE Access

Furthermore, based on EM simulation analysis, we have found that we can approximate the function $f(a;\theta)$ with a Cauchy distribution, as

$$f(a;\theta) = \frac{1}{\pi\Omega}\left[\frac{\Omega^2}{(a-\bar{\mu}(R_l, L_{ex}, \epsilon_r, \theta))^2 + \Omega^2}\right], \quad (6)$$

where Ω shows the scale parameter which specifies the power spread, and $\bar{\mu}(R_l, L_{ex}, \epsilon_r, \theta)$ is the location parameter (peak power location) which can be defined as a function of lens parameters and θ, as

$$\bar{\mu}(R_l, L_{ex}, \epsilon_r, \theta) = a_{\chi+1} + \left(\frac{\theta+\phi}{2\phi}\right)\left(a_{M-\chi} - a_{\chi+1}\right), \quad (7)$$

where ϕ is the maximum field of view of the ULA (i.e., $\pi/3$), and all other parameters are the same as defined earlier. While defining this important lens factor, we assume that, for any AoA θ, the signal energy after passing through the EM lens is focused on a subset of at most $J = 2\chi + 1$ antenna elements. Whereas, we consider $\chi \approx 1, 2, ..., \lll M$ as a known lens focusing design constant which determines the number of antennas under the focused subset area, defined in (1).

Thus, for a certain incident angle θ, the received signal vector obtained at one of the focused subsets of *J* antenna elements, according to expression (2) and (4), is given by $\boldsymbol{z}(t) = [z_{m^*-\chi}(t), \ldots, z_{m^*-1}(t), z_{m^*}(t), z_{m^*+1}(t), \ldots, z_{m^*+\chi}(t)]^T$, where m^* is the peak power bearing antenna location of the subset. Whereas, by using (3), the channel vector $\boldsymbol{h}_p$ for the p^{th} multipath component can be defined as $\boldsymbol{h}_p = [h_{(m^*-\chi)p}, \ldots, h_{(m^*-1)p}, h_{m^*p}, h_{(m^*+1)p}, \ldots, h_{(m^*+\chi)p}]^T$. In this way, once the EM lens-ULA is designed properly and the focusing constant χ is known, the process of selecting the excited subsets of antennas and the estimation of the AoA can be implemented, as discussed in the following section.

IV. ANTENNA SELECTION AND LOCALIZATION

A. ANTENNA SELECTION

From the previous discussions, it can be noted that the EM lens provides the advantage of focusing the received signal on a small subset of antenna elements so that we can process fewer antenna elements per path. Nevertheless, it requires to devise a method to select $S \ll M$ antenna elements (the ones having highest signal energy) without requiring *M* RF chains, as shown in Fig. 4. To perform the optimal antenna selection (AS) process, some schemes are mentioned in [27]–[30] and the references therein. However, in order to select the best optimal subset *S* out of *M* antennas, most of the AS schemes must perform an exhaustive search over $\binom{M}{S}$ possible options. This may raise the order of complexity for large *M* and moderate *S*. Our proposed method is particularly well suited for the AS process. In this subsection, we describe two types of simplified AS approaches using RF switches:

1) subset based AS for fully digital BB high-resolution subspace based AoA estimation algorithms (i.e., MUSIC, Root MUSIC and ESPRIT), and
2) RF coupler based AS for mixed analog-digital based AoA estimation techniques (e.g., $\sum -\Delta$ patterns).

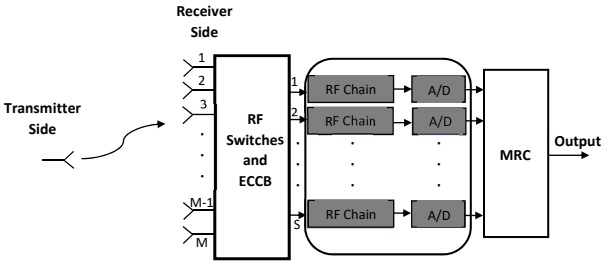

FIGURE 4: Overview of the traditional antenna selection method.

1) Subset Based AS

Let us consider a vector corresponding to the excited subset of antennas indexes denoted by $\boldsymbol{j}_p \subset \bar{\boldsymbol{m}}$ for a path *p*, where the size of $\boldsymbol{j}_p$ is equal to J. Whereas, $\bar{\boldsymbol{m}}$ is a vector of indexes of size M that denotes all the excited and non-excited antenna elements signals of the ULA. Furthermore, since the received signal power in the focused subset is unevenly distributed, the maximum power, according to expression (7), is obtained by the subset's central antenna element, marked with m^*. In this way, we can select $\boldsymbol{j}_p$ out of *M* antennas by searching the peak power bearing antenna m^* of the subset with an optimized threshold $\mathcal{T}$. Once, the peak power location m^* of a subset is identified, all other excited antennas of that subset can be identified by selecting $\mid m - m^*(\theta) \mid \leq \chi$ elements. The task of sweeping across the ULA can be done by low powered high speed RF switches, controlled by the electronic control circuit board (ECCB) block (Fig. 1). Note that for this AS technique we can ignore the coupler component branches shown in Fig. 1. Moreover, for identifying the m^* antenna, we can define the average signal-to-noise ratio (SNR) of the received signal on the m^{th} antenna element (γ_m), as

$$\gamma_m = \frac{\rho}{\sigma^2}|h_m|^2, \quad (8)$$

where, ρ is the signal power. In this manner, we summarize the AS process as follows, where card(.) represents the number of members in a set.

Algorithm 1 Subset Based AS

1: Define two sets, initially, one for the selected antennas $\hat{\mathcal{M}} = \emptyset$ and other for the unselected antennas $\mathcal{U} = \{1, \ldots, M\}$.
2: Initialize a variable $N_P = 0$ to count the number of multipath components.
3: **while** $\left(Card(\hat{\mathcal{M}}) \leq S\right)$ **do**
4: Perform: $m^* = \max_{m \in \mathcal{U}} [\gamma_m \geq \mathcal{T}]$.
5: Extract: $\boldsymbol{j}_p = \mid m - m^* \mid \leq \chi$ antennas of a subset of size J.
6: Modify: $\hat{\mathcal{M}} = \hat{\mathcal{M}} \cup \{\boldsymbol{j}_p\}$ and $\mathcal{U} = \mathcal{U} \backslash \{\boldsymbol{j}_p\}$.
7: Update: $N_P = N_P + 1$.
end

This article has been accepted for publication in a future issue of this journal, but has not been fully edited. Content may change prior to final publication. Citation information: DOI 10.1109/ACCESS.2019.2891110, IEEE Access

It should be noted that the signals selected are the BB converted and digitally processed.

2) RF Coupler Based AS

In order to perform the AoA estimation with a mixed analog-digital structure, and with reduced computational complexity, we propose a simple AS technique based on $180°$ hybrid rat race (HRR) coupler followed by an integrator and comparator as shown in Fig. 1. This technique considers that the signal arriving from path *p* is focused on at least one coupler branch. A coupler branch includes a pair of two antennas connected to the coupler, an integrator that computes the signal energy, and a comparator to compare the received signal energy with a preset threshold (V_{Th}). In this way, initially, the signal is processed by the HRR coupler. The coupler generates the $\sum$ and Δ patterns of the two input signals, namely, $m_{\sum}$ and m_{Δ}, respectively, where $m_{\sum} \in [1, 3, 5, \ldots, M-1]$ and $m_{\Delta} = m_{\sum}+1 \in [2, 4, 6, \ldots, M]$, and M is an even number. More details about the HRR coupler and $\sum -\Delta$ patterns can be found in [31], [32].

After obtaining the $\sum -\Delta$ patterns from one of the excited subset's branched coupler, the $\sum$-pattern from the $m_{\sum}$ port element is passed through the integrator and comparator in order to check if the obtained signal energy $\left(\hat{\gamma}_{m_{\sum}} = \int |z_{m_{\sum}}(t)|^2 dt\right)$ exceeds V_{Th}. Once it exceeds V_{Th}, both $\sum -\Delta$ pattern ports of the p^{th} path ($m^*_{\sum,p}$ and $m^*_{\Delta,p}$) are selected by the ECCB block with the help of low powered high speed RF switches for further processing. Whereas, RF switches are swept across maximum *M*/2 couplers. Note that V_{Th} can be considered in the interval $\mathcal{T} < V_{Th} < 2\mathcal{T}$. In this way, we can summarize the RF coupler based AS technique as follows, where, $m^*_{\sum,p}$ and $m^*_{\Delta,p}$, respectively, represent the two antenna ports indexes which contain the $\sum -\Delta$ patterns of path *p*.

Algorithm 2 RF Coupler Based AS

1: Define two sets, initially, one for the selected antennas $\hat{\mathcal{M}} = \emptyset$ and another for the unselected antennas $\mathcal{U} = \{1, \ldots, M\}$.
2: Initialize a variable $N_P = 0$ to count the number of multipath components.
3: **while** $\left(Card(\hat{\mathcal{M}}) \leq S\right)$ **do**
4: **if** $\left(\hat{\gamma}_{m_{\sum}} \geq V_{Th}\ AND\ m \in \mathcal{U}\right)$ **then**
5: Perform: $m^*_{\sum,p} = m_{\sum}$
6: $m^*_{\Delta,p} = m_{\Delta} = m_{\sum} + 1$.
7: Extract: $\boldsymbol{j}_p = \{m^*_{\sum,p}, m^*_{\Delta,p}\}$ antennas.
8: Modify: $\hat{\mathcal{M}} = \hat{\mathcal{M}} \cup \{\boldsymbol{j}_p\}$ and $\mathcal{U} = \mathcal{U} \backslash \{\boldsymbol{j}_p\}$.
9: Update: $N_P = N_P + 1$.
end
end

B. LOCALIZATION PROCEDURE

In order to estimate the angular location of the received signal in a fixed observation time window, the selected antenna's signals are advanced to the localization/processor block which performs two steps. In the first step, it detects the FAP signal based on computing the ToA of each path (excited subset). We assume that the FAP is the direct path (LoS) and contains the AoA information which belongs to the actual direction of the user terminal. In the second step, the estimated FAP signal is supplied to the AoA estimation algorithm in order to estimate the location of the user. Therefore, in following subsections, we describe these two steps.

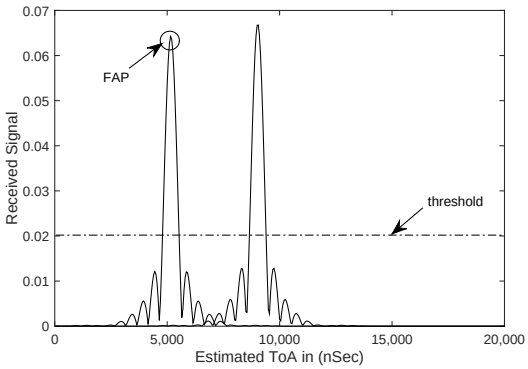

FIGURE 5: An example of ToA estimation based FAP detection in the proposed system.

1) FAP Signal Detection

In order to detect the FAP signal, we propose to use the correlation based ToA estimation technique. It appears a simple and good choice in our proposed system where multipath components are considered spatially separated on different subsets of antennas as a function of the angle of incidence. More details about general working principles of correlation based ToA estimation can be found in [33].

Thus, in the proposed method with multipath propagation, the BS must find the first arriving path and its time delay, rather than finding the highest peak of the correlation. This is because it is not always true that the direct path signal will be the strongest. Therefore, the arriving peak of each focused subset's signal is estimated by comparing the absolute value of the correlator output with a certain defined threshold according to the measured noise power, as shown in Fig. 5 as one of the examples of finding the ToA of two focused subsets signals. In this way, we select that peak among all estimated N_p peaks whose time delay (τ_p) is the minimum, where $\tau_0 < \tau_1, < \ldots, < \tau_{N_P-1}$ and τ_0 denotes the delay for the FAP. We summarize the algorithm for FAP signal detection in Algorithm 3.

2) Lens Based AoA Estimation

The identified FAP signal vector $\boldsymbol{r}(t)$ is further processed by the AoA estimation block to find the AoA of the source signal. In this regard, many AoA estimation algorithms exist in the literature such as the Bartlett method, Capon's method, multiple signal classification (MUSIC), joint angle and delay estimation (JADE)-MUSIC, estimation of signal parameter

This article has been accepted for publication in a future issue of this journal, but has not been fully edited. Content may change prior to final publication. Citation information: DOI 10.1109/ACCESS.2019.2891110, IEEE Access

Algorithm 3 FAP Signal Detection

1: Define a set for the estimated ToAs of N_P focused subsets as $\mathcal{I}_{peaks} = \{\emptyset\}$.
2: Initialize a variable $p = 1$.
3: **while** $\left(p \leq card\left(\hat{\mathcal{M}}\right)/N_P\right)$ **do**
4: Calculate the power of each selected subset's signal vector $\boldsymbol{z}_p(t)$ corresponding to $\boldsymbol{j}_p \in \hat{\mathcal{M}}$ selected antenna indexes, as $\rho_{z,p} = sum(abs(\boldsymbol{z}_p(t)^2)/length(\boldsymbol{z}_p(t)))$.
5: Measure the noise power of $\boldsymbol{z}_p(t)$ to fix threshold, as $\rho_{n,p} = \sqrt{2}/2 * 10^{(-SNR/20)} * \sqrt{\rho_{z,p}}$.
6: Perform correlation between $\boldsymbol{z}_p(t)$ and $\boldsymbol{s}(t)$ $\widetilde{z}_p = \times corr\left(\boldsymbol{z}_p(t), \boldsymbol{s}(t)\right)$.
7: Find maximum peak's ToA of $\widetilde{z}_p$ satisfying $\rho_{n,p}$ and update $\mathcal{I}_{peaks}$, as $\mathcal{I}_{peaks} = \mathcal{I}_{peaks} \cup \max\{find(|\widetilde{z}_p| > \rho_{n,p})\}$.
8: $p = p + 1$.
end
9: Extract the ToA of the FAP (τ_0) from vector $\mathcal{I}_{peaks}$ as $\tau_0 = \min(\mathcal{I}_{peaks})$.
10: Extract the FAP subset signal from $\hat{\mathcal{M}}$ selected antennas using the index of $\mathcal{I}_{peaks}$ corresponding to τ_0, as
$\boldsymbol{r}(t) = \boldsymbol{z}_0(t)$, for subset based AS,
$\boldsymbol{r}(t) = [\sum_0(t), \Delta_0(t)]$, for coupler based AS,
where, $\sum_0(t)$ and $\Delta_0(t)$ are the sum and difference patterns of the FAP, respectively.

via rotational invariance technique (ESPRIT), Root-MUSIC, and $\sum -\Delta$ patterns [33]–[37]. However, as mentioned earlier, we will discuss and apply the subspace-based high resolution (MUSIC, Root MUSIC and ESPRIT) and $\sum -\Delta$ patterns-based techniques in combination with the EM lens assisted massive antennas array in order to investigate their performance. Additionally, as a benchmark, we also consider the JADE-MUSIC algorithm in the case of w/o lens for the comparison with our approach. The EM lens based subspace AoA estimation algorithms are explained in [17], [38]. It can be noticed from these references that by using the EM-lens enabled subsets based AS (Algorithm 1), the dimension of the covariance matrix and the corresponding EVD is reduced from $M \times M$ (w/o lens) to $J \times J$, where $J \lll M$, which consequently minimizes the computational costs of the signal processing. Furthermore, we describe the $\sum -\Delta$ patterns AoA estimation technique in the following subsection.

a: Sum ($\sum$) - Difference (Δ) Patterns Technique

The $\sum -\Delta$ patterns method is a simple and low complexity based AoA estimation technique which can fit well in our proposed system. In principle, it can be implemented by using two antennas after identifying the FAP. Here, unlike the subspace-based methods, we do not need to form the covariance matrices and the corresponding EVD to estimate the AoA. Instead, the two signals received on two antenna elements, spaced from each other by distance *d*, are used to take their sum and difference. Then, by computing the ratio of Δ to $\sum$ patterns, the AoA can be estimated with significantly less computational cost.

Initially, let us assume that each incoming multipath component of a source signal is focused on a distinct small subset of antennas on the ULA. In this way, the signal from a focused subset of antennas is passed through the coupler (s), as shown in Fig. 1. Thus, the coupler generates the $\sum$ and Δ patterns of the two input antennas incident signal of path *p* at its two output ports, respectively, as

$$\sum\nolimits_p(t) = z_m(t) + z_{m+1}(t), \tag{9}$$

$$\Delta_p(t) = z_m(t) - z_{m+1}(t). \tag{10}$$

Then, by using the coupler based AS (Algorithm 2), those $\sum -\Delta$ ports (i.e., $m^*_{\sum,p}$ and $m^*_{\Delta,p}$) that satisfy the fixed threshold are selected. Additionally, using Algorithm 3, a pair of $\sum -\Delta$ ports excited by the FAP signal is chosen. It contains the sum and difference patterns, i.e., $\sum_0(t)$, and $\Delta_0(t)$ of the FAP signal. It can be proved that by taking the ratio of expression (10) to (9) for the FAP signal, at time instant *t*, we can arrive at the following expression

$$\frac{\Delta_0}{\sum_0} = \frac{1 - e^{j\kappa d \sin\theta_p}}{1 + e^{j\kappa d \sin\theta_p}}, \tag{11}$$

where $\kappa = 2\pi/\lambda_0$ is the wave number. Finally, we can estimate the AoA $\hat{\theta}_0$ of the FAP signal as follows

$$\hat{\theta}_0 = \sin^{-1}\left\{\frac{\lambda_0}{\pi d}\tan^{-1}\left(real\left(-j\frac{\Delta_0}{\sum_0}\right)\right)\right\}, \tag{12}$$

where tan^{-1} and *real* show the inverse of tangent function and real part of the argument, respectively. The proof of expressions (9) through (12) is provided in Appendix B. Note that the ratio $\frac{\Delta_0}{\sum_0}$ could also be achieved by using an analog RF-divider component followed by a processor to compute (12). Thus, the coupler makes it possible to implement the $\sum$-Δ patterns technique in a simplified mixed analog-digital structure without using frequency down converters.

V. NUMERICAL RESULTS

In this section, by considering experimental parameters, we report some simulation results for the AoA estimation performance, and hardware and computational complexity reduction analysis of the proposed method using the subspace and $\sum -\Delta$ patterns based techniques. We also investigate the performance analysis of these algorithms in terms of the root mean squared error (RMSE) in degrees, which is defined as

$$RMSE = \sqrt{\mathbb{E}\left[|\theta_0 - \hat{\theta}_0|^2\right]}, \tag{13}$$

where θ_0 is the actual angle and $\hat{\theta}_0$ shows the estimated AoA of the FAP. We consider a well-known JADE-MUSIC algorithm as a reference method for the comparison with our proposed method. One can find details about this method in [39], [40]. The following main steps can be taken into account while implementing the JADE-MUSIC [41]: frame

This article has been accepted for publication in a future issue of this journal, but has not been fully edited. Content may change prior to final publication. Citation information: DOI 10.1109/ACCESS.2019.2891110, IEEE Access

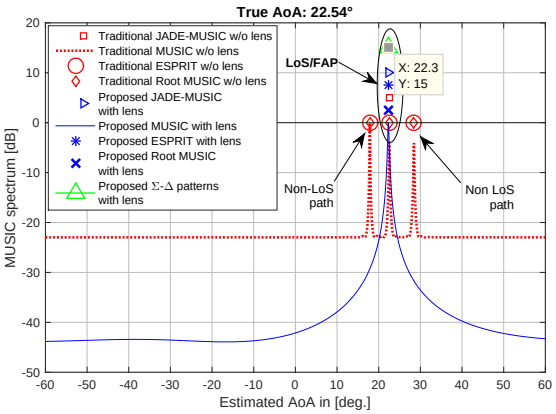

FIGURE 6: Estimated AoA using different techniques with lens versus w/o lens.

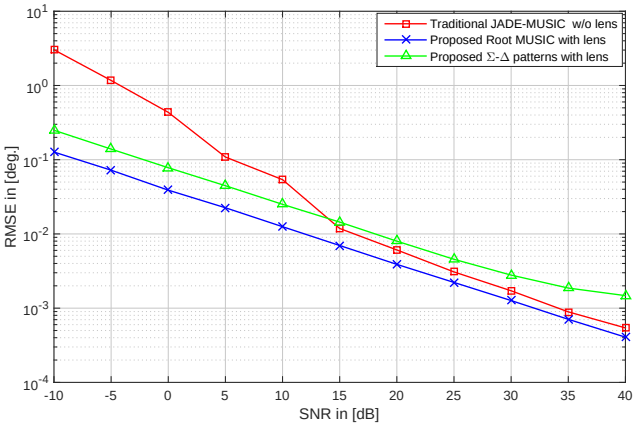

FIGURE 7: RMSE performance as a function of the *SNR* in dB with lens versus w/o lens.

synchronization to coarsely identify the frame position, channel impulse response estimation, formation of covariance matrix from the estimated channel responses of each antenna (with size MN, where N represents the discrete Fourier transform points) and computation of the 2-D MUSIC spectrum in both the spatial and temporal domains.

A. AOA ESTIMATION PERFORMANCE

Initially, we assume that a single user terminal's signal arrives at the BS via a LoS path (θ_0, τ_0) and N_P=2 multipaths which are spatially separated at least by $\sigma_\eta = \pm 5°$. Hence, according to N_P, the θ_p's and τ_p's are randomly generated for the multipath signals according to our defined signal model in Section III. Moreover, we consider a BS consisting of a lens ($R_l = 25\lambda_0$) combined with an ULA of M=100 elements with inter-antenna spacing d=λ_0/2. Due to the practical limitation of the antenna array, the angle coverage of the ULA is set to $\phi = \pi/3$ so that $\theta_p \in [-\pi/3, \pi/3]$. Additionally, we use the EM lens based signal model given in (2) by setting the lens focusing design constant χ=1 so that J=3 antenna elements are illuminated in a subset. The SNR is set to 15dB.

Having outlined the initial assumed parameters, in Fig. 6, we show the estimated AoA with lens versus w/o lens using the subspace (i.e., MUSIC, Root MUSIC and ESPRIT) and $\sum -\Delta$ patterns algorithms. It can be observed from the results that the estimated AoA with the lens case is in good agreement to the w/o lens case. Moreover, in the lens case, the $\sum -\Delta$ patterns technique provides identical results with significantly reduced computational complexity as compared to the subspace-based algorithms.

In Fig. 6, we also display the AoA for the non-LoS multipath arrivals in the case of w/o lens when subspace-based methods are applied. These interfering multipath arrivals in the w/o lens system can not be isolated using the traditional subspace-based methods. Hence, these methods are mapped into the joint angle and delay estimation (JADE)-algorithm which provides both ToA and AoA information of each path [33] and facilitates the extraction of the AoA of the FAP. Nevertheless, the computational complexity of the JADE type algorithm is significantly higher than the traditional subspace-based methods. Thus, we considered the JADE-MUSIC method [39], [40] in the w/o lens system in order to make the comparison with our proposed approach. It can be observed that the estimated AoA with EM lens is in good agreement with the one provided by the high resolution and complicated JADE-MUSIC algorithm w/o lens system. Note that the hardware and complexity of the JADE-MUSIC w/o lens system is described and compared with the lens system in the next subsection.

Furthermore, we now discuss the RMSE performance results of the proposed approach by using the conventional subspace, and $\sum -\Delta$ patterns techniques. Since the Root MUSIC method's performance is slightly better than the MUSIC and ESPRIT, we consider only the Root MUSIC. We average all the estimated results over 10^4 realizations of randomly generated AoAs.

Fig. 7 shows the RMSE as a function of the *SNR* in dB for both systems (with lens versus w/o lens), while keeping all other parameters constant as mentioned earlier. Here, the estimated RMSE performance of the lens system, especially using the Root MUSIC method is improved, particularly at *SNR*$\leq$20 dB, as compared to w/o lens system using the JADE-MUSIC algorithm. While both systems perform almost identically as the *SNR* increases, after 20 dB. Furthermore, the $\sum -\Delta$ technique also performs well as compared to w/o lens system at lower *SNR*, i.e., $\leq$10 dB. However, in the lens case when *SNR*$\leq$30dB, the Root MUSIC performs better (around 5 dB) as compared to the $\sum -\Delta$ technique. This is because, per excited subset, the $\sum -\Delta$ method considers a smaller number of antennas (two antennas) as compared to the subspace-based method which utilizes three antennas in the excited subset and performs the covariance and EVD operations. Note that the lens system uses three antennas per multipath component at most. This is in sharp

This article has been accepted for publication in a future issue of this journal, but has not been fully edited. Content may change prior to final publication. Citation information: DOI 10.1109/ACCESS.2019.2891110, IEEE Access

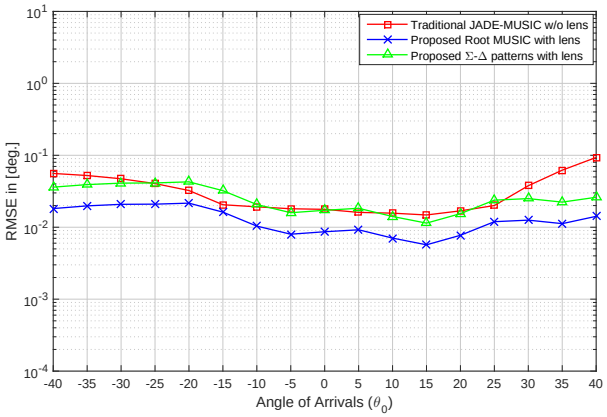

FIGURE 8: RMSE performance as a function of the AoA (θ_0) with lens versus w/o lens.

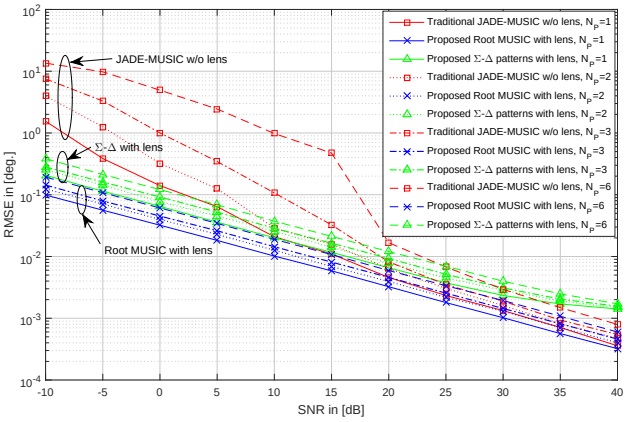

FIGURE 9: RMSE performance as a function of the *SNR* in dB at different number of N_P multipath signals.

contrast to the w/o lens system which utilizes all *M=100* antennas/RF chains and implements a highly complicated JADE-MUSIC algorithm.

Furthermore, we investigate the RMSE performance as a function of the AoA (θ_0) in both systems, with lens and w/o lens, by fixing the *SNR* to 15 dB. The obtained RMSE graph is illustrated in Fig. 8. The RMSE results with the lens case using Root MUSIC are improved as compared to the w/o lens case which faces more interference from multiple signal components. Moreover, the $\sum -\Delta$ method also provides comparable results.

In Fig. 9, we show the RMSE performance as a function of the *SNR* in dB for different number of multipath (N_P) signal components and arbitrary angular separation among them. It can be remarked that at lower values of *SNR* ($\leq$20 dB), the performance improvements in the lens system with Root MUSIC are apparent while as the *SNR* and N_P increase, both systems, with and w/o lens, tend to achieve similar performance results. Additionally, the $\sum -\Delta$ technique also provides comparable results that are slightly less in resolution compared to the lens based Root MUSIC method, but better than w/o lens system, particularly at lower *SNR* values, i.e., *SNR*$\leq$10 dB. While, for further increased *SNR*, for instance *SNR*$>$30 dB, $\sum -\Delta$ does not improve the performance.

In this way, we further assume different sized subsets for the focused antennas, i.e., χ in the lens case while keeping all other parameters constant. For the w/o lens case, we also consider a different number of antennas as $\mathcal{M} = 2\chi + 1$. Hence, we calculate and show the RMSE as a function of χ for both cases (with lens versus w/o lens) in Fig. 10. Here we can observe that at different values of χ, the obtained results with the lens system, particularly at lower values of χ, are improved as compared to the case w/o the lens due to the additional interference rejection gain provided by the lens system by focusing each multipath component signal on distinct subset of antennas. Moreover, such performance improvement can also be realized when the same lens system is used for the data transfer application as illustrated in Fig.

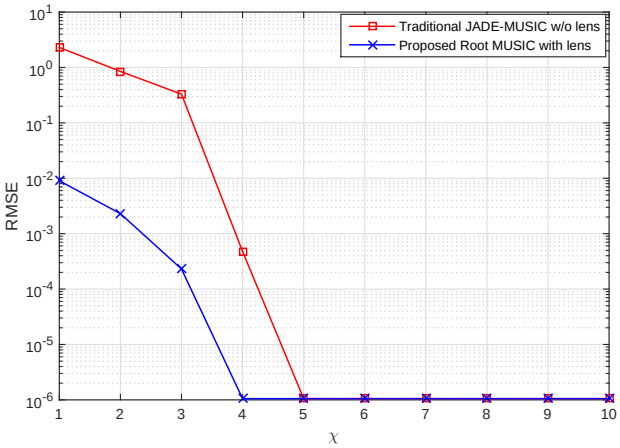

FIGURE 10: RMSE performance as a function of χ number of antenna elements.

11. Whereas we show the average received *SNR* at the array output as a function of the training/transmission *SNR* (ρ_{tr}- the ratio of the transmitted power to the noise power) for a user terminal with its estimated/known AoA. It can be observed that the results obtained with lens look prominent over the w/o lens case particularly for ρ_{tr} less than 10 dB. Note that here we considered *M*=100 antennas, $\chi = 2$ and all other parameters/mathematical expressions as mentioned in the EM lens related work done in [11].

B. COMPLEXITY AND HARDWARE REDUCTION ANALYSIS

In the traditional w/o lens MAA system, the subspace-based methods, i.e., 2-D JADE-MUSIC, need to estimate the covariance matrix that involves a computational complexity on the order of $O\left(MN_{samp}\right)^3$. Furthermore, it also needs to perform the EVD with $O\left(MN_{samp}\right)^3$, and compute the spectrum on $(180/\Delta_\phi)N_{samp}$ points, where Δ_ϕ and

This article has been accepted for publication in a future issue of this journal, but has not been fully edited. Content may change prior to final publication. Citation information: DOI 10.1109/ACCESS.2019.2891110, IEEE Access

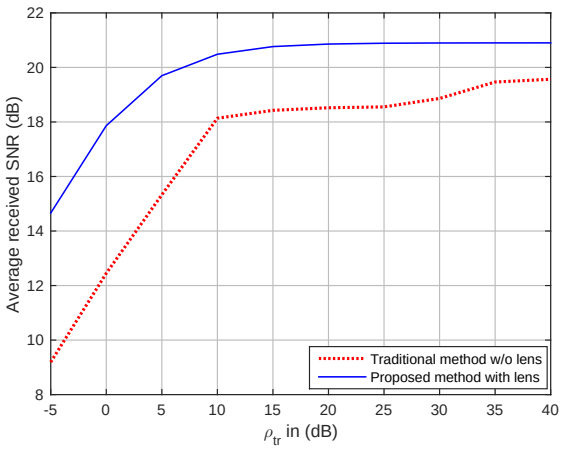

FIGURE 11: Performance of average received *SNR* as a function of ρ_{tr} for the two systems with lens and w/o lens.

N_{samp} represent the desired angular resolution (in degrees) and number of samples/snapshots of the received signal, respectively [41]. The hardware components cost include the *M* number of operational antennas and the same *M* number of RF chains to process the signals in BB. In contrast, the EM lens assisted MAA system performs the localization with one of the subspace-based methods, i.e., 1-D MUSIC, that involves significantly reduced computational complexity. It involves the complexity of the AS, the FAP detection, the computation of the covariance and EVD matrices on the order of $O\binom{M}{N_P J}, O\left(J^2 N_P\right), O\left(JN_{samp}\right)^3$, and $O\left(JN_{samp}\right)^3$, respectively, whereas, $J \ll M$. Moreover, after the FAP subset detection, the hardware components include a very low number of active antennas such as *J* out of *M* antennas of the ULA and correspondingly *J* number of RF chains to process a signal.

Furthermore, the mixed analog-digital based $\sum -\Delta$ technique in the case of w/o lens system, involves the computational complexity of $O\left(2M\right)$ for the single source and LoS scenario [42]. However, according to the related work reported in [41], the complexity can be higher in the case of multipath channels since it requires to perform the fast Fourier transforms, recursive least square channel estimation, and fine-synchronization (inverse FFT with search for the minimum), respectively, with complexity on the order of $O\left(MN_{samp}log_2 N_{samp}\right)$, $O\left(MN_{samp}\right)$, $O\left(MN_{samp}log_2 N_{samp}\right)$, and $O\left(N_{samp}\right)$. Additionally, the hardware requirements include *M* antennas, M/2 analog components (i.e., HRR couplers, integrators and comparators) and correspondingly M number of RF chains. In contrast, the $\sum -\Delta$ technique with the lens based MAA system mainly involves the computational complexity of the AS, the FAP detection, and the processing of two signal patterns (e.g., $\sum$ and Δ corresponding to the two antennas excited by the FAP), respectively, on the order of $O\binom{M/2}{2N_P}, O\left(2^2 N_P\right)$, and $O(2)$. Moreover, the hardware comprises M/2 analog components (i.e., HRR couplers, integrators and comparators), two FAP operational antennas out of M, and correspondingly two RF chains to process a FAP signal.

VI. CONCLUSION

In this paper, we proposed and analyzed a simplified system for radio source localization using an EM lens MAA. Firstly, we discussed the lens antennas system model and studied the focusing ability of the lens antennas as a function of the lens geometric parameters and angle of incidence. This focusing ability of the lens opens the door to localization systems based on MAA technology. This approach allows to simplify the system complexity with good performance results. Secondly, by combining the EM lens with a MAA, we presented an approach for localization based on AoA estimation in multipath channels using a subsets/coupler based antenna selection, ToA estimation based FAP detection, and different AoA estimation algorithms. We investigated the performance of the subspace and $\sum -\Delta$ patterns based methods with lens antennas using the fully digital and mixed analog-digital structures, respectively, and compared them to the w/o lens system which utilizes the high resolution JADE-MUSIC algorithm. The localization results obtained by employing the EM lens are in good agreement to the conventional system w/o the lens with, however, significantly reduced complexity. Hence, the proposed approach has a great potential for application to next generation 5G wireless systems.

.

APPENDIX A DESIGN PARAMETERS OF PATCH ANTENNAS

In Table 1, the design parameters assumed for the two QWT patch antennas are provided. The antennas are integrated with the Si and Qu lenses in the EM simulations. Note that the relative permittivity constant (ϵ_r) of the antennas substrates are closer to the dielectric constants of the assumed lenses in order to reduce the reflections.

TABLE 1: Design parameters of QWT matched patch antennas in millimeter (mm) unit using Rogers RO3210 (Si lens) and RO3035 (Qu lens) substrates.

Substrate	Rogers RO3210	Rogers RO3035
Substrate permitivity (ϵ_r)	10.2	3.5
tanD loss ($tan\delta$)	0.0027	0.0015
Substrate height (h_{sub})	0.5	0.5
Patch width	8.56	11.46
Patch length	4.29	7.61
QWT width	0.1818	0.54
QWT length	3.13	3.13
Substrate width	11.6	14.46
Substrate length	10.55	13.87
Copper thickness	0.017	0.017

This article has been accepted for publication in a future issue of this journal, but has not been fully edited. Content may change prior to final publication. Citation information: DOI 10.1109/ACCESS.2019.2891110, IEEE Access

APPENDIX B PROOF OF $\sum - \Delta$ PATTERNS BASED AOA ESTIMATION

Let us assume that we have already selected the FAP signal subset and we input the coupler with a signal coming from two antennas (z_{m^*} and z_{m^*+1}). The coupler will generate the $\sum$ and Δ patterns at its two output ports. The $\sum_0(t)$ and $\Delta_0(t)$ patterns of the FAP signal at $\sum$-port $\left(m^*_{\sum}\right)$ and Δ-port $\left(m^*_{\Delta} = m^*_{\sum} + 1\right)$ can be expressed as

$$\sum\nolimits_0(t) = \boldsymbol{r}_1(t) = z_{m^*}(t) + z_{m^*+1}(t), \tag{14}$$

or, by using expression (2) and neglecting the noise component, we get

$$\sum\nolimits_0(t) = \sqrt{\alpha_0}\exp\left(j\psi_0 + j\kappa d m^* \sin\theta_0\right)\Big[P_{m^*}(\theta_0) + P_{m^*+1}(\theta_0)\exp\left(j\kappa d\sin\theta_0\right)\Big]s(t-\tau_0). \tag{15}$$

Similarly, for Δ-port, we have

$$\Delta_0(t) = \boldsymbol{r}_2(t) = z_{m^*}(t) - z_{m^*+1}(t), \tag{16}$$

or,

$$\Delta_0(t) = \sqrt{\alpha_0}\exp\left(j\psi_0 + j\kappa d m^* \sin\theta_0\right)\Big[P_{m^*}(\theta_0) - P_{m^*+1}(\theta_0)\exp\left(j\kappa d\sin\theta_0\right)\Big]s(t-\tau_0). \tag{17}$$

where $\kappa = 2\pi/\lambda_0$, and $\boldsymbol{r}_1(t)$ and $\boldsymbol{r}_2(t)$, respectively, represent the first and second element of the FAP signal vector $\boldsymbol{r}(t)$ given in Algorithm 3. In this way, at particular time instant t, by taking the ratio Δ_0 to $\sum_0$, we get

$$\frac{\Delta_0}{\sum_0} = \frac{P_{m^*}(\theta_0) - P_{m^*+1}(\theta_0)\exp\left(j\kappa d\sin\theta_0\right)}{P_{m^*}(\theta_0) + P_{m^*+1}(\theta_0)\exp\left(j\kappa d\sin\theta_0\right)}. \tag{18}$$

By assuming $\frac{P_{m^*}(\theta_0)}{P_{m^*+1}(\theta_0)} \approx 1$, the expression in (18) becomes

$$\begin{aligned}\frac{\Delta_0}{\sum_0} &= \frac{1 - \exp\left(j\kappa d\sin\theta_0\right)}{1 + \exp\left(j\kappa d\sin\theta_0\right)} \\ &= \frac{\exp\left(\frac{-j\kappa d\sin\theta_0}{2}\right) - \exp\left(\frac{j\kappa d\sin\theta_0}{2}\right)}{\exp\left(\frac{-j\kappa d\sin\theta_0}{2}\right) + \exp\left(\frac{j\kappa d\sin\theta_0}{2}\right)}(Euler's form) \\ &= j\tan\left(\frac{\kappa d\sin\theta_0}{2}\right).\end{aligned} \tag{19}$$

Thus, we can obtain the estimated AoA $\hat{\theta}_0$, as

$$\hat{\theta}_0 = \sin^{-1}\left\{\frac{\lambda_0}{\pi d}\tan^{-1}\left(real\left(-j\frac{\Delta_0}{\sum_0}\right)\right)\right\}. \tag{20}$$

ACKNOWLEDGMENT

The authors wish to acknowledge the Higher Education Commission of Pakistan and the OeAD-Austria for the support of Sarmad Shaikh with the scholarship to carry out the PhD at the University of Klagenfurt, Austria.

REFERENCES

[1] J.Thornton and K. Huang, Modern Lens Antennas for Communications Engineering. IEEE Press, John Wiley and Sons, Inc., Hoboken, New Jersey, 2013.

[2] D. F. Filipovic, S. S. Gearhart, and G. M. Rebeiz, "Double-slot antennas on extended hemispherical and elliptical silicon dielectric lenses," IEEE Transactions on Microwave Theory and Techniques, vol. 41, no. 10, pp. 1738–1749, 1993.

[3] T. H. Buttgenbach, "An improved solution for integrated array optics in quasi-optical mm and submm receivers: the hybrid antenna," IEEE Transactions on Microwave Theory and Techniques, vol. 41, no. 10, pp. 1750–1760, 1993.

[4] E. Larsson, O. Edfors, F. Tufvesson, and T. Marzetta, "Massive MIMO for next generation wireless systems," IEEE Communications Magazine, vol. 52, no. 2, pp. 186–195, February 2014.

[5] A. Gupta and R. K. Jha, "A survey of 5G network: Architecture and emerging technologies," IEEE Access, vol. 3, pp. 1206–1232, 2015.

[6] T. S. Rappaport, S. Sun, R. Mayzus, H. Zhao, Y. Azar, K. Wang, G. N. Wong, J. K. Schulz, M. Samimi, and F. Gutierrez, "Millimeter wave mobile communications for 5G cellular: It will work!" IEEE Access, vol. 1, pp. 335–349, 2013.

[7] K. T. Jo, Y. C. Ko, C. G. Park, and J. S. Park, "Multiple-antenna post low noise amplifier RF combining," in Proc. of IEEE GLOBECOM Workshops, Nov 2009, pp. 1–5.

[8] X. Gao, O. Edfors, F. Tufvesson, and E. Larsson, "Massive MIMO in real propagation environments: Do all antennas contribute equally?" IEEE Transactions on Communications, vol. 63, no. 11, pp. 3917–3928, Nov 2015.

[9] S. A. Shaikh and A. M. Tonello, "Localization based on angle of arrival in EM lens-focusing massive MIMO," in Proc. of IEEE 6th International Conference on Consumer Electronics (ICCE), Berlin, Germany, September 2016, pp. 124–128.

[10] D. Inserra and A. M. Tonello, "Characterization of hardware impairments in multiple antenna systems for doa estimation," Journal of Electrical and Computer Engineering, pp. 1–10, 2011.

[11] Y. Zeng, R. Zhang, and Z. N. Chen, "Electromagnetic lens-focusing antenna enabled massive MIMO performance improvement and cost reduction," IEEE Journal on Selected Areas in Communications, vol. 32, no. 6, pp. 1194–1206, June 2014.

[12] ——, "Electromagnetic lens focusing antenna enabled massive MIMO," in Proc. of IEEE CIC International Conference on Communications (ICCC), Aug 2013, pp. 454–459.

[13] H. C. So, Y. T. Chan, and F. K. W. Chan, "Closed-form formulae for time-difference-of-arrival estimation," IEEE Transactions on Signal Processing, vol. 56, no. 6, pp. 2614–2620, June 2008.

[14] A. Tonello and D. Inserra, "Radio positioning based on DoA estimation: An implementation perspective," in Proc. of IEEE International Conference on Communications (ICC) Workshops, June 2013, pp. 27–31.

[15] D. Inserra and A. Tonello, "A multiple antenna wireless testbed for the validation of DoA estimation algorithms," International Journal of Electronics and Communications, vol. 68, no. 1, pp. 10–18, January 2014.

[16] D. Laurijssen, J. Steckel, and M. Weyn, "Antenna arrays for RSS based indoor localization systems," in IEEE SENSORS 2014 Proceedings, Nov 2014, pp. 261–264.

[17] S. A. Shaikh and A. M. Tonello, "DoA estimation in EM lens assisted massive antenna system using subsets based antenna selection and high resolution algorithms," International Journal of Radioengineering, vol. 27, no. 1, pp. 159–168, April 2018.

[18] R. Shafin, L. Liu, and J. Zhang, "DoA estimation and RMSE characterization for 3D massive-MIMO/FD-MIMO OFDM system," in Proc. of IEEE Global Communications Conference (GLOBECOM), December 2015, pp. 1–6.

[19] A. Wang, L. Liu, and J. Zhang, "Low complexity direction of arrival (DoA) estimation for 2D massive MIMO systems," in Proc. of IEEE Globecom Workshops, December 2012, pp. 703–707.

[20] F. Shu, Y. Qin, T. Liu, L. Gui, Y. Zhang, J. Li, and Z. Han, "Low-complexity and high-resolution DOA estimation for hybrid analog and digital massive MIMO receive array," IEEE Transactions on Communications, vol. 66, no. 6, pp. 2487–2501, 2018.

[21] N. Garcia, H. Wymeersch, E. G. Larsson, A. M. Haimovich, and M. Coulon, "Direct localization for massive MIMO," IEEE Transactions on Signal Processing, vol. 65, no. 10, pp. 2475–2487, May 2017.

This article has been accepted for publication in a future issue of this journal, but has not been fully edited. Content may change prior to final publication. Citation information: DOI 10.1109/ACCESS.2019.2891110, IEEE Access

[22] X. Lan, L. Wang, Y. Wang, C. Choi, and D. Choi, "Tensor 2-D DOA estimation for a cylindrical conformal antenna array in a massive MIMO system under unknown mutual coupling," IEEE Access, vol. 6, pp. 7864–7871, 2018.
[23] H. Huang, J. Yang, H. Huang, Y. Song, and G. Gui, "Deep learning for super-resolution channel estimation and DOA estimation based massive MIMO system," IEEE Transactions on Vehicular Technology, vol. 67, no. 9, pp. 8549–8560, Sept 2018.
[24] V. Savic and E. Larsson, "Fingerprinting-based positioning in distributed massive MIMO systems," in Proc. of IEEE Vehicular Technology Conference (VTC Fall), Boston, MA, September, 2015, pp. 1–5.
[25] T. K. Nguyen, T. A. Ho, H. Han, and I. Park, "Numerical study of self-complementary antenna characteristics on substrate lenses at terahertz frequency," Journal of Infrared, Millimeter, and Terahertz Waves, vol. 33, no. 11, pp. 1123–1137, 2012.
[26] W. L. Stutzman and G. A. Thiele, Antenna Theory and Design. John Wiley and Sons Inc, Newyork, 1998.
[27] S. Sanayei and A.Nosratinia, "Antenna selection in MIMO systems," IEEE Communication Magazine, vol. 1, pp. 34–37, 2012.
[28] A. Lu and V. Lau, "Phase only RF precoding for massive MIMO systems with limited RF chains," IEEE Transactions on Signal Processing, vol. 62, no. 17, pp. 4505–4515, 2014.
[29] M. Al-Shuraifi and H. Al-Raweshidy, "Optimizing antenna selection using limited CSI for massive MIMO systems," in IEEE Proceedings, 74(7), 2014, pp. 180–184.
[30] Y. Zeng and R. Zhang, "Cost-effective millimeter-wave communications with lens antenna array," IEEE Wireless Communications, vol. 24, no. 4, pp. 81–87, 8 2017.
[31] S. A. Shaikh and A. M. Tonello, "Performance analysis of 180 degree HRR coupler used for direction finding with an antenna array," International Journal of Online Engineering (iJOE), vol. 13, no. 10, pp. 86–102, October 2017.
[32] ——, "Complexity reduced direction finding massive MIMO system using EM lens," in IRACON-COST International Workshop on Dependable Wireless Communications and Localization for the IoT, TU Graz University, Graz, Austria, September 2017, pp. 1–3.
[33] S. A. R. Zekavat and R. M. Buehrer, Handbook of Position Location. IEEE Press, John Wiley and Sons, Inc. Hoboken, New Jersey, 2012.
[34] B. Allen and M. Ghavami, Adaptive Array Systems. John Wiley and Sons Inc., England, 2005.
[35] I. A. H. Adam and M. D. R. Islam, "Perfomance study of direction of arrival (DOA) estimation algorithms for linear array antenna," in Proc. of International Conference on Signal Processing Systems, May 2009, pp. 268–271.
[36] S. A. Shaikh and I. Tekin, "Two axis direction finding antenna system using sum-difference patterns in X-band," Microwave and Optical Technology Letters, vol. 57, no. 9, pp. 2085–2092, September 2015.
[37] K. Witrisal and et al, "Whitepaper on new localization methods for 5G wireless systems and the internet-of-things," a project of IRACON, pp. 1–25, April 2018.
[38] S. A. Shaikh and A. M. Tonello, "Em lens-clustering based direction of arrival estimation in massive antenna systems," in Proc. of IEEE International Conference on Smart Systems and Technologies (SST), Osijek, Croatia, October 2017, pp. 127–131.
[39] R. Feng, Y. Liu, J. Huang, J. Sun, C. Wang, and G. Goussetis, "Wireless channel parameter estimation algorithms: Recent advances and future challenges," IEEE China Communications, vol. 15, no. 5, pp. 211–228, May 2018.
[40] M. C. Vanderveen, C. B. Papadias, and A. Paulraj, "Joint angle and delay estimation (JADE) for multipath signals arriving at an antenna array," IEEE Communications Letters, vol. 1, no. 1, pp. 12–14, Jan 1997.
[41] D. Inserra and A. M. Tonello, "A frequency-domain LOS angle-of-arrival estimation approach in multipath channels," IEEE Transactions on Vehicular Technology, vol. 62, no. 6, pp. 2812–2818, 2013.
[42] R. Y. Q. Zhu, S. Yang and Z. Nie, "Direction finding using multiple sum and difference patterns in 4D antenna arrays," Hindawi-International Journal of Antennas and Propagation, vol. 2014, pp. 1–13, 2014.

SARMAD A. SHAIKH (first author) was born in Pakistan. He received the PhD in Information Technology from the University of Klagenfurt, Klagenfurt, Austria in September 2018, the M.S. Electronics Engineering degree from Sabanci University, Istanbul, Turkey in 2015, and the B.S. Telecommunication Engineering degree from FAST-NUCES, Pakistan in 2011. Currently, he is working as an Assistant Professor in the department of Avionics Engineering at Pakistan Air Force-Karachi Institute of Economics and Technology (PAF-KIET), Karachi, Pakistan. His research interests include RF/microwave engineering, radio source localization and antenna (EM lens antenna) array designing.

ANDREA M. TONELLO (M'00–SM'12) was born in Italy. He received the laurea degree in electrical engineering (summa cum laude) and the Ph.D in electronics and telecommunications from the University of Padova, Padova, Italy, in 1996 and in 2002, respectively. From 1997 to 2002, he was with Bell Labs-Lucent Technologies, Whippany, NJ, USA, first as a Member of the Technical Staff. Then, he was promoted to Technical Manager and appointed to Managing Director of the Bell Labs Italy division. In 2003, he joined the University of Udine, Udine, Italy, where he became Aggregate Professor in 2005 and Associate Professor in 2014. Currently, he is Professor at the Chair of Embedded Communication Systems of the University of Klagenfurt, Klagenfurt, Austria. Dr. Tonello received several awards, including the Distinguished Visiting Fellowship from the Royal Academy of Engineering, U.K., in 2010, the IEEE Distinguished Lecturer Award from VTS in 2011-2015 and from COMSOC in 2018-2019, and nine best paper awards. He was the Chair of the IEEE Communications Society Technical Committee on Power Line Communications and was/is Associate Editor of several journals including IEEE Trans. on Vehicular Technology, IEEE Trans. on Communications, and IEEE Access. He served as general chair or TPC co-chair of several conferences among which IEEE ISPLC 2011 and IEEE SmartGridComm 2014.